



Diurnal Asymmetry Effects of Photovoltaic Power Plants on Land Surface Temperature in Gobi Deserts

Xubang Wang ¹, Qianru Zhou ¹, Yong Zhang ¹, Xiang Liu ¹, Jianquan Liu ¹, Shengyun Chen ^{1,2}, Xinxin Wang ³ and Jihua Wu ^{1,*}

- ¹ State Key Laboratory of Herbage Improvement and Grassland Agro-Ecosystems, College of Ecology, Lanzhou University, Lanzhou 730000, China; 220220932481@lzu.edu.cn (X.W.); 220220932780@lzu.edu.cn (Q.Z.); 120220907681@lzu.edu.cn (Y.Z.); lx@lzu.edu.cn (X.L.); liujq@lzu.edu.cn (J.L.); sychen@lzb.ac.cn (S.C.)
- ² State Key Laboratory of Cryospheric Science, Northwest Institute of Eco-Environment and Resources, Chinese Academy of Sciences, Lanzhou 730000, China
- ³ Ministry of Education Key Laboratory for Biodiversity Science and Ecological Engineering, National Observations and Research Station for Wetland Ecosystems of the Yangtze Estuary, Institute of Biodiversity Science and Institute of Eco-Chongming, School of Life Sciences, Fudan University, Shanghai 200438, China
- * Correspondence: wjh@lzu.edu.cn

Abstract: The global expansion of photovoltaic (PV) power plants, especially in ecologically fragile regions like the Gobi Desert, highlights the suitability of such areas for large-scale PV development. The most direct impact of PV development in the Gobi Desert is temperature change that results from the land-use-induced albedo changes; however, the detailed and systemic understanding of the effects of PV expansion on land surface temperature remains limited. This study focuses on the 16 largest PV plants in the Chinese Gobi Desert, utilizing remote sensing data to assess their effects on land surface temperature. Our result showed a cooling effect during the daytime (-0.69 ± 0.10 °C), but a warming effect during the nighttime (0.23 ± 0.05 °C); the overall effect on the daily mean was a cooling effect (-0.22 ± 0.05 °C). Seasonal variations were observed, with the most significant cooling effect in autumn and the weakest in summer. The PV area was the most significant factor which influenced the temperature variation across PV plants. Our findings enrich our understanding of the environmental effects arising from the construction of PV plants and provide vital information for the design and management of increasingly renewable electricity systems globally.

Keywords: remote sensing; diurnal variability; land surface temperature; MODIS; solar energy



Citation: Wang, X.; Zhou, Q.; Zhang, Y.; Liu, X.; Liu, J.; Chen, S.; Wang, X.; Wu, J. Diurnal Asymmetry Effects of Photovoltaic Power Plants on Land Surface Temperature in Gobi Deserts. *Remote Sens.* **2024**, *16*, 1711.

<https://doi.org/10.3390/rs16101711>

Received: 2 March 2024

Revised: 30 April 2024

Accepted: 9 May 2024

Published: 11 May 2024



Copyright: © 2024 by the authors. Licensee MDPI, Basel, Switzerland. This article is an open access article distributed under the terms and conditions of the Creative Commons Attribution (CC BY) license (<https://creativecommons.org/licenses/by/4.0/>).

1. Introduction

Greenhouse gas emissions from fossil fuels are responsible for ~75% of the global “heat pollution” leading to rising temperatures across the globe [1]. To achieve the goal of limiting global temperature increase, a variety of mitigation strategies are needed, including substantial increase in the production of renewable energy. Among renewable energy sources, PV solar energy technology is among the most promising due to its exceptional cleanliness [2], widely available resources [3], and consistently declining costs [4]. From 2009, the global capacity for PV power generation has been expanding rapidly [5], with the global cumulative installed capacity for PV power generation projected to grow to 4240 GW by 2040 [5]. The growth of solar power in China outstrips that of any other country in the world, and its total installed PV capacity increased from 100 MW in 2007 to 205,000 MW in 2019, with a compound annual growth rate of 79.8% since 2007 [6]. As of 2021, China accounted for 36% of the global solar capacity [7].

The rapid expansion of PV power plants has created a new type of land-use change [8] that leads to changed local microclimates (e.g., temperature and moisture) by altering photosynthetic active radiation and surface albedo [9–11]. These microclimatic changes

could, in turn, induce changes in the ecosystem, for example, in the form of altered vegetation, plant and soil biodiversity, and soil carbon cycling [12–14]. Changes to land surface temperature (LST) are particularly important because it is related to near-surface and underground processes that directly influence ecosystem functions [15,16] but can also influence ecosystems indirectly via soil moisture–temperature feedbacks [17]. Countries such as the United States, India, and China are currently experiencing or have already undergone a booming phase in PV energy [5], which is predicted to induce environmental impacts. Thus, a deeper understanding of the impact of large-scale PV power plants on LST is crucial in order to assess environmental (e.g., local climate) and ecological (e.g., plant phenology, biodiversity) impacts of large-scale PV deployment [18,19].

While some studies have shown a cooling effect of PV power plants on LST [20–23], others have reported warming effects [12,24,25]. These inconsistent results may stem from the fact that these local-scale studies differ in the time data collected, as well as in the climate and ecosystem types in which the studies took place [26,27]. Furthermore, because of a lack of long-term monitoring data, it is difficult to compare temperatures near PV plants with pre-construction conditions [22,25,28]. Even when model-based large-scale analyses are used, the parameters are mainly derived from individual locations and not universal [9,29,30].

The Gobi Desert, mainly located in northern China and southern Mongolia in East Asia, is experiencing rapid expansion of PV power plants because of its low cloud cover, abundant solar radiation, and cheap land resources [31]. By 2019, the area covered by PV in Northwestern China had nearly tripled compared to 2013, with PV in the Gobi Desert accounting for 37% of that change [32,33]. At the same time, the Gobi Desert is an ecologically fragile ecosystem characterized by high variable microclimatic conditions, low plant cover, and low biodiversity [34,35]. However, previous studies on the influence of PV plants in the Gobi Desert have mainly relied on field observations and model simulations [16,36]. Remote sensing based on satellite data has been widely applied to measure heat- and cool-island effects caused by land use changes [37,38] and offers a potential large-scale means of quantifying the LST changes caused by PV power plants [16]. Compared to in situ field observation, remote sensing technology allows the comparison and analysis of temperature data before and after the construction of PV power plants. Previous studies which used remote sensing data to study the effects of PV power plants on LST were limited to single-site [11] or covered multiple ecosystem types [39]. Therefore, the detailed and systemic understanding of the effects of PV expansion on LST in the Gobi Desert of China remains limited.

Here, in this study, we use satellite-derived remote sensing data of LST to quantitatively analyze the effects of large PV power plants on LST in the Gobi Desert in northwestern China. We specifically ask the following questions: (1) Is there a temporal difference (i.e., daily or seasonally) in the impact of PV power plant construction on LST? (2) What are the major factors influencing the impact of PV power plants on LST in the Gobi Desert?

2. Materials and Methods

2.1. Dataset Sources

Since Gobi PV plants are mainly located in northwestern China, we used the dataset released by Xia et al. [32] (accessible at <https://code.earthengine.google.com/d6f17fa4fa44639db580d5f8b196fa5b>, accessed on 6 April 2023.) to acquire data on the PV distribution in 2019, which consists of a 30 m resolution PV panel map of northwestern China. The map was developed by integrating a multiresolution segmentation algorithm, the object-based classification (ISOC) algorithm, and Landsat imagery within Google Earth Engine. This map includes a total of 885 PV panels in northwestern China, 95 PV plants of which occurred within the Gobi Desert.

We obtained remotely sensed LST data from the MODIS (Moderate-Resolution Imaging Spectroradiometer) Terra and Aqua satellites, characterized by a spatial resolution of 1 km. The LST data obtained from MODIS are one of the most extensively used LST prod-

ucts [40,41] and are derived from clear-sky observations with a 99% confidence level [42]. Two datasets were chosen (Terra and Aqua), which locally pass the equator at 10:30 and 22:30 local time for Terra and 1:30 and 13:30 local time for Aqua every day, ensuring that our LST data accurately reflect the local LST of PV plants [43,44]. In this study, we used MOD11A1.006 [43] and MYD11A1.006 [44] from the Google Earth Engine platform (<https://code.earthengine.google.com/>, accessed on 24 May 2023.).

We obtained land cover data in 2018 from the 30 m Land Use and Land Cover (LULC) dataset of China (obtained from the Data Center for Resources and Environmental Sciences, Chinese Academy of Sciences; <https://www.resdc.cn/DOI/DOI.aspx?DOIID=54>, accessed on 3 May 2023.).

We used the local climate conditions, such as annual mean temperature (MAT), annual precipitation (MAP), solar radiation (Rs), wind speed (Ws), and water vapor pressure (Vp) for each plant. We downloaded the 30 arc seconds (about 1 km) climate data from the WorldClim (version 2.1) dataset [45].

2.2. Selection of PV Power Plants in Gobi Deserts

To evaluate the influence of PV power plants on temperature and other variables in the Gobi Desert, we used the following steps: (1) We first generated a 1 km buffer zone based on the periphery of the PV panels (grid) and merged overlapping buffer zones into one entity, defining it as a PV power plant (area within the green boundary) (Figure 1b). We used a 1 km buffer because the effect of PV panels on LST can extend up to 730 m [16]. In total, we calculated the area (km²) of 358 PV panels taken from 885 panels. (2) From those 95 Gobi Desert PV plants, we selected 16 where the PV panel area is greater than 3 km², and the plant area is greater than 20 km² (Table S1 and Figure 1a). The 16 selected plants contain between 31 (Hami-East plant) and 226 (Golmud plant) 1 km × 1 km LST data grids (Figure S1). We used Google Earth satellite imagery to evaluate when the PV plant construction at all sites was initiated and completed (Figure 1c). All the above steps were processed using Python code [46] and Google Earth Pro [47].

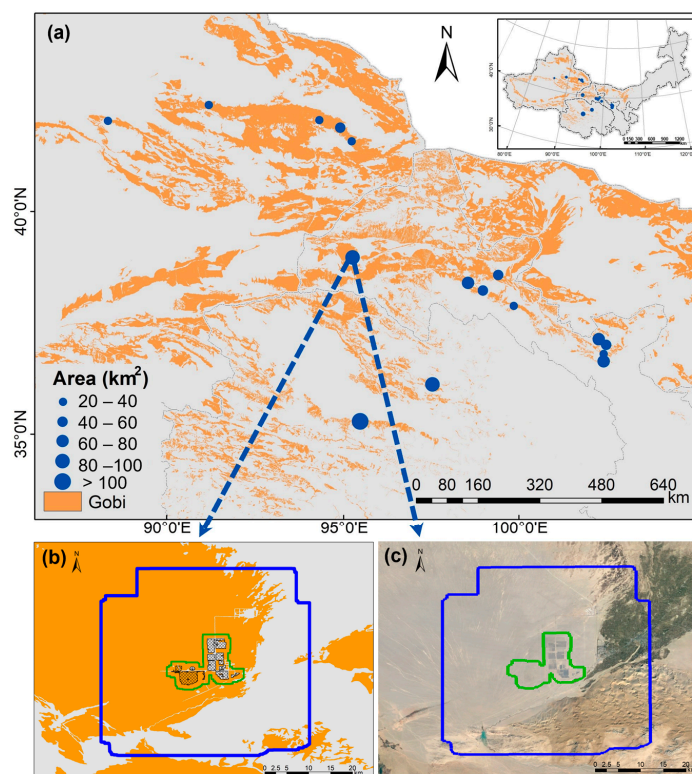


Figure 1. Study area. (a) Location of the Gobi region and photovoltaic power plants in China;

(b) Dunhuang PV power plant; (c) Google Earth satellite imagery of Dunhuang PV power plant. The green line and blue line in (b,c) indicate in (1 km buffer) and out (15 km buffer) of the Dunhuang plant.

2.3. Quantifying the Impact of PV Plants on LST

We obtained both daytime and nighttime LST data from the 16 designated PV plants and calculated their monthly and annual means by using the Google Earth Engine platform. To do so, we first established a 1 km buffer based on the PV panels to represent the plant's area. Then, we applied a supplementary buffer of 15 km to represent the area outside of the plant (i.e., the control) (Figure 1b,c). After that, we calculated the difference in the LST between the inside and outside of the plant for the three years immediately prior to plant construction and the first three years after construction to quantify the effect of PV plants on LST [39,48]. The specific formula we used for these calculations is as follows:

$$\Delta LST = \Delta LST_{In} - \Delta LST_{Out} = LST_{In(After-Before)} - LST_{Out(After-Before)} \quad (1)$$

where ΔLST represents the land surface temperature variation in the PV power plants. "In" and "Out" refer to the LST data inside and outside the PV power plant, respectively. "After" and "Before" correspond to the three years data after and before the construction of the PV power plant, respectively. ΔLST_{In} and ΔLST_{Out} represent the inside and outside change in LST ($^{\circ}C$) before and after the construction of PV power plant, respectively. The detailed procedures of this study are shown in Figure 2.

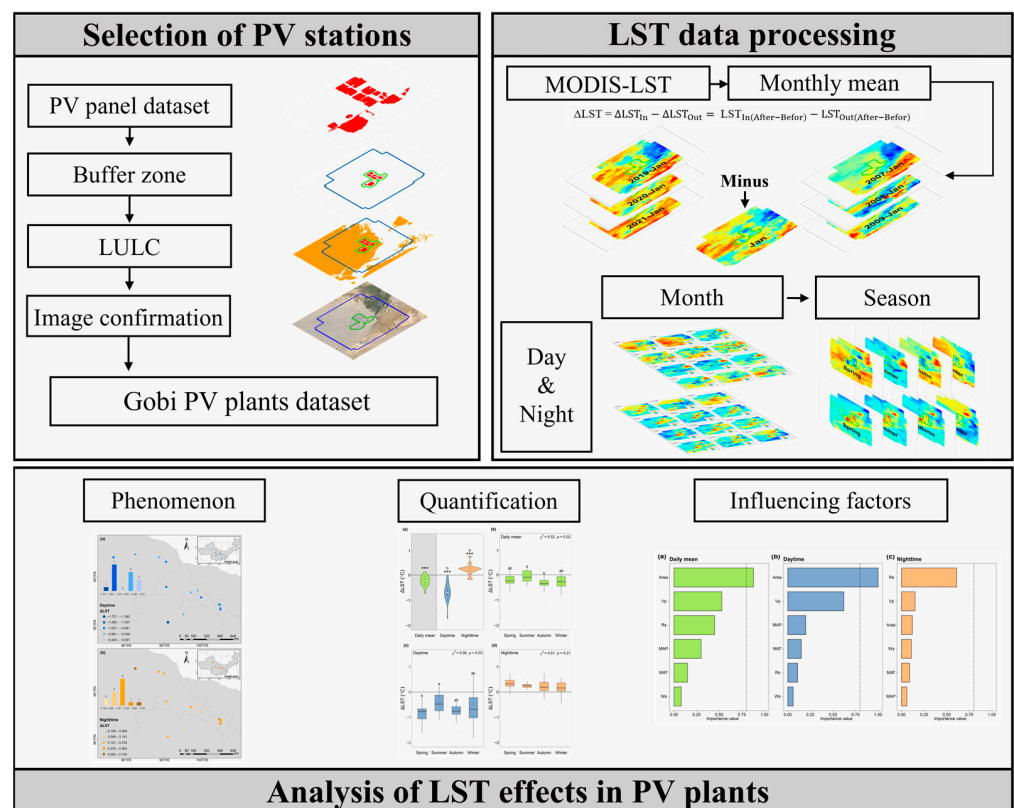


Figure 2. Workflow of this study. In the top left image, the red rectangle represents the PV panel, the green and blue lines represent the buffer, and the orange color represents the Gobi surface. In the top right image, the colored image represents LST data. In the lower image, ***: statistically significant at $p < 0.001$ levels.

We used one-sample t -test to examine if the LST in each diurnal period significantly differs from zero ($\mu = 0$) across all plants. To assess the difference in LST between daytime and nighttime periods, we employed independent two-sample t -test. Due to the non-

normality of the autumn data, seasonal variations were tested by Kruskal–Wallis analysis and Dunn’s test as a post hoc analysis to investigate pairwise differences among seasons. All analyses were conducted using R statistical software version 4.2.0 [49].

2.4. Effects of Different Factors on the LST of PV Power Plant

We performed model selection to identify predictive variables largely influencing the impact of PV power plants on LST. Candidate predictors included area (Area), annual mean temperature (MAT), annual precipitation (MAP), solar radiation (Rs), wind speed (Ws), and water vapor pressure (Vp) (Table S2). We constructed linear models with all abovementioned predictors as full models for different diurnal periods. All variables in the full model were standardized using the “standardize” function in the arm package [50]. Subsequently, we generated a subset of models based on the full models, ranked by the Akaike information criterion corrected for small sample sizes (AICc), the difference in AICc of the given model from the minimum-AICc model (ΔAICc), and the model weights (wAICc), using the “dredge” function in the MuMIn package [51]. The wAICc weighted average standardized coefficients for models with $\Delta\text{AICc} < 4$ were calculated as the effect size of each predictive variable, using the “model.avg” function in the MuMIn package [51]. Ultimately, effect size indicates how much the dependent variable is expected to change when the independent variable changes. The sign of the effect size shows the direction of the influence: positive means a positive effect, and negative means a negative effect. Statistical significance is indicated when the 95% confidence interval of the effect size does not include zero. All analyses used R statistical software version 4.2.0 [49].

3. Results

3.1. Diurnal Fluctuations in PV Power Plants Effects on LST

We first illustrate the effect of PV power plants on LST using the Dunhuang plant as an example (see detailed information in Supplementary Materials), showing daytime cooling but nighttime warming effects on LST. This phenomenon was general across all PV plants (Figure 3), which are individually shown in Figure 4. During the daytime, all plants exhibited a cooling effect; half of the plants showed a cooling effect $>1^\circ\text{C}$ on the annual LST change. We found that all but two plants warmed during nighttime; the other two had slight cooling. Out of those plants with nighttime warming, 10 of the 16 plants experienced warming effects $>0.19^\circ\text{C}$. Overall, there was a significant reduction in daily mean LST due to PV power plants of $-0.23 \pm 0.05^\circ\text{C}$ (mean \pm SE) (t -test, $t_{15} = -4.46$, $p < 0.001$). During the daytime, there was a significant decline in annual LST $-0.69 \pm 0.10^\circ\text{C}$ (t -test, $t_{15} = -7.02$, $p < 0.001$), whereas the annual LST increased by $0.22 \pm 0.05^\circ\text{C}$ (t -test, $t_{15} = 4.25$, $p < 0.001$) during nighttime (Figure 5a).

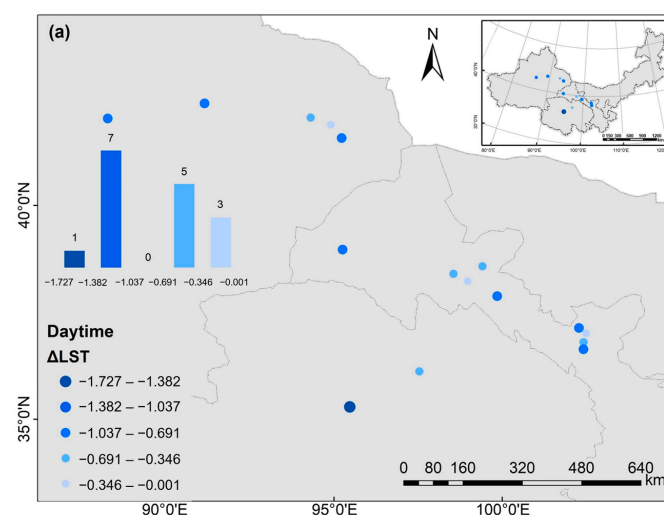


Figure 3. Cont.

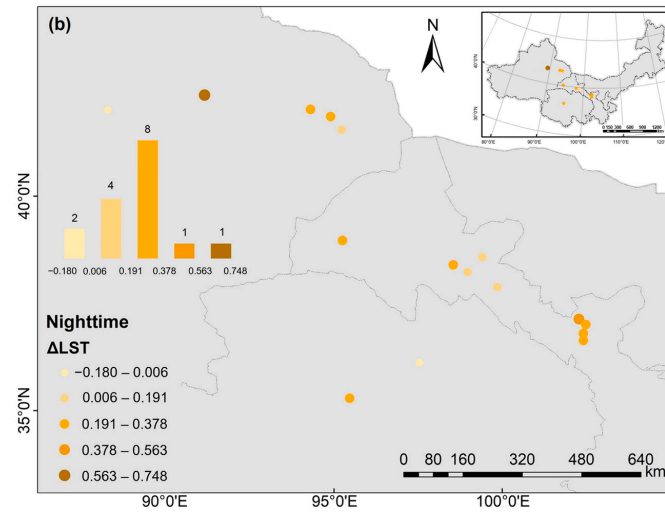


Figure 3. Effects of photovoltaic power plant on LST of (a) daytime period and (b) nighttime period.

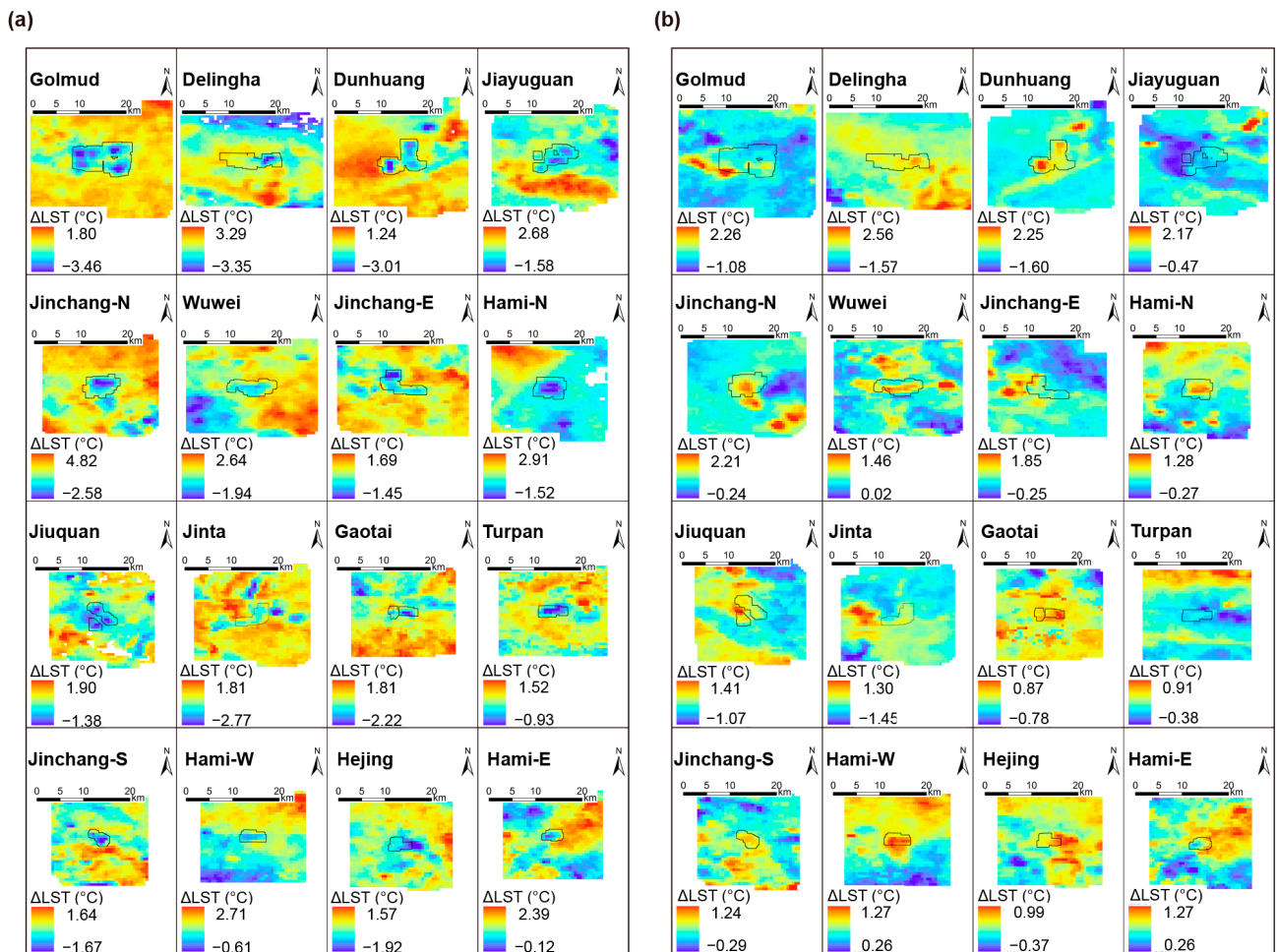


Figure 4. The PV power plant effects on the annual means of LST of (a) daytime period and (b) nighttime period in all photovoltaic power plants, the black line represents the extent of the PV plant.

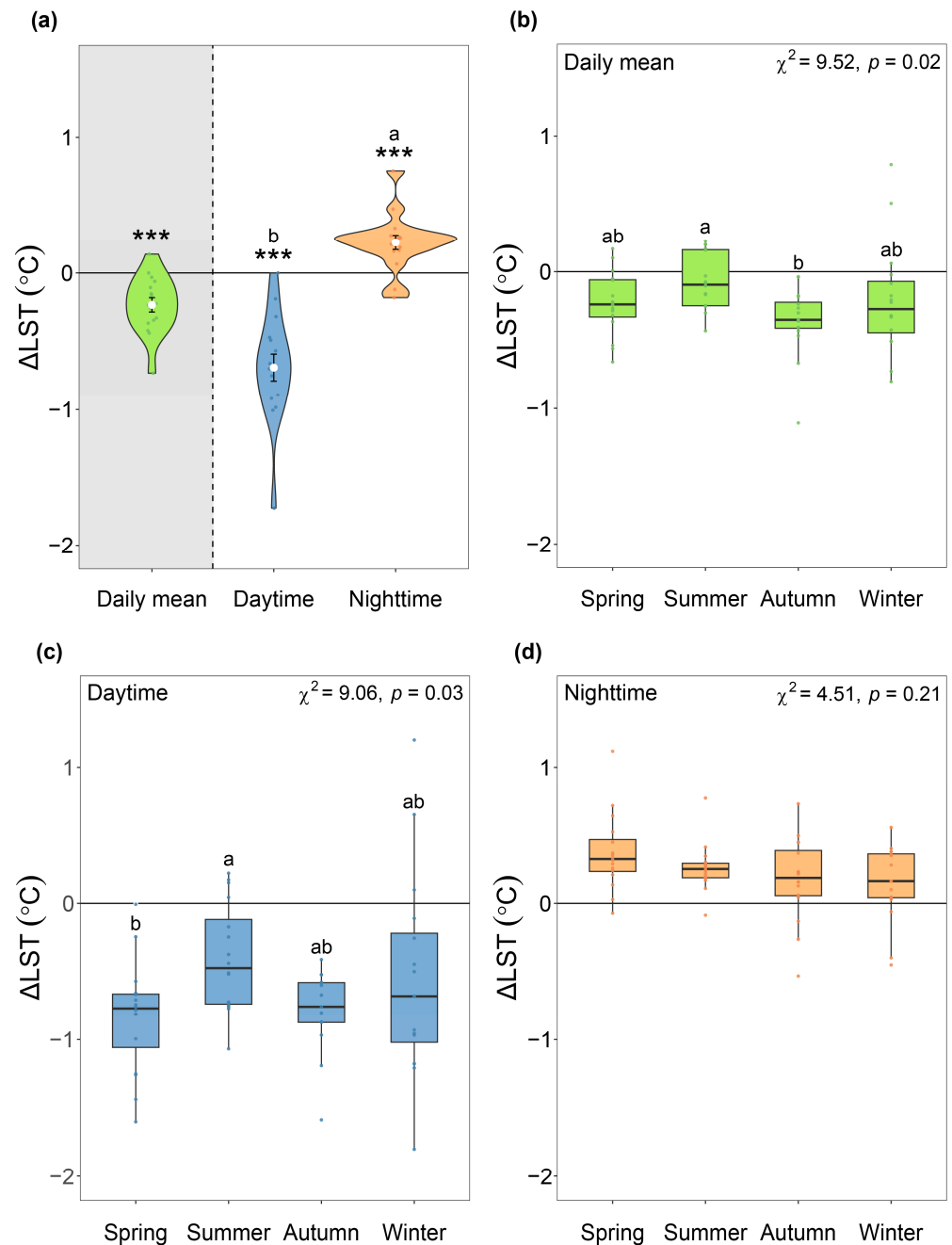


Figure 5. Effect of photovoltaic power plants on LST across all plants. (a) Diurnal variations in effects (Δ LST); the background violin plot characterizes the distribution of plants in each diurnal period effect, while white dots represent the mean value. Statistical difference was tested by one-sample *t*-test between each period effect and zero ($\mu = 0$) and independent two-sample *t*-test between daytime and nighttime period. ***: statistically significant at $p < 0.001$ levels, respectively. Seasonal variation in effects (Δ LST) separated into (b) daily mean, (c) daytime period, and (d) nighttime period. Statistical difference was tested by Kruskal–Wallis analysis and Dunn’s test as a post hoc analysis to investigate pairwise differences between seasons. The boxes represent the interquartile range, the lines inside the boxes represent the medians, and the whiskers denote the lowest and highest values within 1.5 times the interquartile range. Lowercase letters denote significant differences between seasons. Colored dots represent each plant data.

3.2. Seasonal Fluctuations in PV Power Plants Effects on LST

We explored the effects of PV power plants on monthly LST (Figure 6). We found that the daily mean LST changes cooled (Δ LST < 0) for all months except for June and

July, which exhibited a slight warming effect ($\Delta\text{LST} > 0$) (Figure 6a). The extent of cooling varied across the year, ranging from the least in January to the most in October. During the daytime, the highest cooling effect ($\Delta\text{LST} < 0$) was observed in October. Conversely, during the nighttime, the highest warming effect ($\Delta\text{LST} > 0$) was during June.

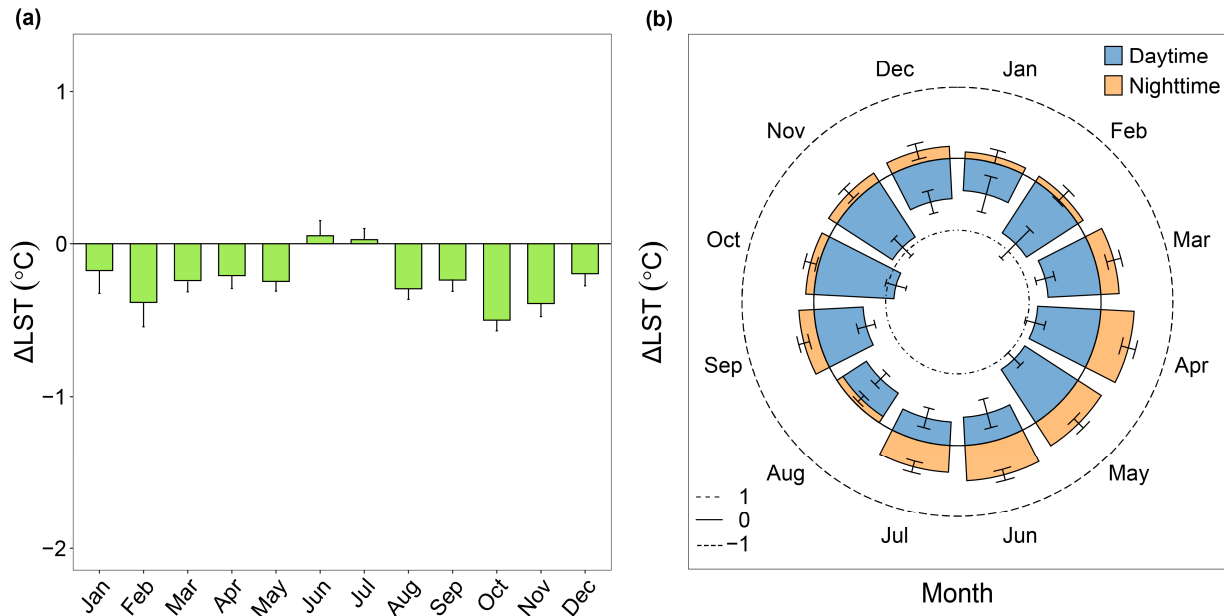


Figure 6. Effects of PV power plant on monthly LSTs across all plants, separated into (a) daily mean and (b) daytime and nighttime period.

We also evaluated the effects of seasonal variation in PV power plants on LST using four distinct seasons: spring (March–May), summer (June–August), autumn (September–November), and winter (December–February). Here, we found that daily mean LST exhibited cooling effects ($\Delta\text{LST} < 0$) with the strongest effect in autumn; only the differences between summer and autumn are significant (Figure 5b). Daytime LST changes showed cooling effects ($\Delta\text{LST} < 0$), especially in the spring and autumn; the significant differences between seasons only occur between spring and summer (Figure 5c). The strongest cooling effect was in spring and the weakest in summer, consistent with the trend seen in the daily mean. Nighttime LST changes were consistently warming ($\Delta\text{LST} > 0$) (Figure 5d). The warming effect was strongest in spring and weakest in winter.

3.3. Factors Influencing the PV Power Plant Effects on LST

We explored the diverse factors that influence the effects induced by PV power plants on LST through model averaging after model selection (Figures 7 and 8). The effect on daily mean temperature was negatively associated with area and water vapor pressure (Figure 7a) and showed a marginally positive correlation with solar radiation (Table S3, $p = 0.068$). During daytime, the PV power plant effect was significantly associated with area, water vapor pressure, and wind speed. Specifically, there was a positive correlation with wind speed and a negative correlation with area and water vapor pressure (Figure 7b). During nighttime, the PV power plant effect was only marginally correlated with solar radiation (Figure 7c, Table S3, $p = 0.080$).

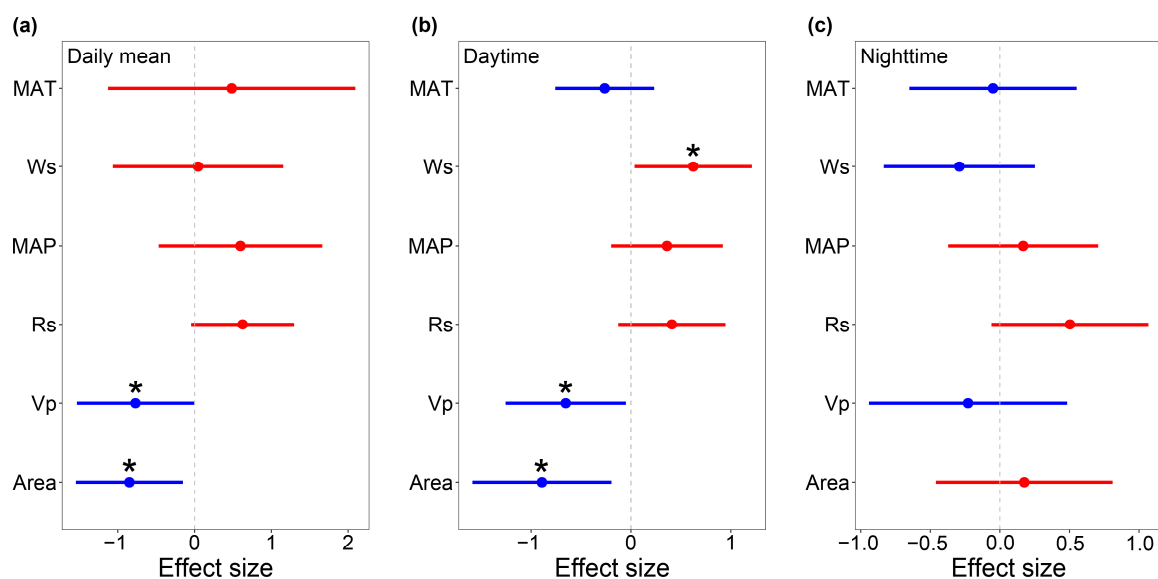


Figure 7. Factors that influenced the effects of PV power plant on LST, include area, mean annual temperature (MAT), mean annual precipitation (MAP), solar radiation (Rs), wind speed (Ws), and water vapor pressure (Vp). Estimate effect sizes with 95% confidence intervals are derived from the weighted average standardized coefficients of models with $\Delta AICc < 4$. The relative importance of factors on (a) daily mean, (b) daytime period, and (c) nighttime period, as estimated by linear models. Blue lines indicate negative effects, and red lines indicate positive effects. *: statistically significant at $p < 0.05$ level. Model-averaged importance of the predictors and the p -value of each factor are shown in Figure 8 and Table S3.

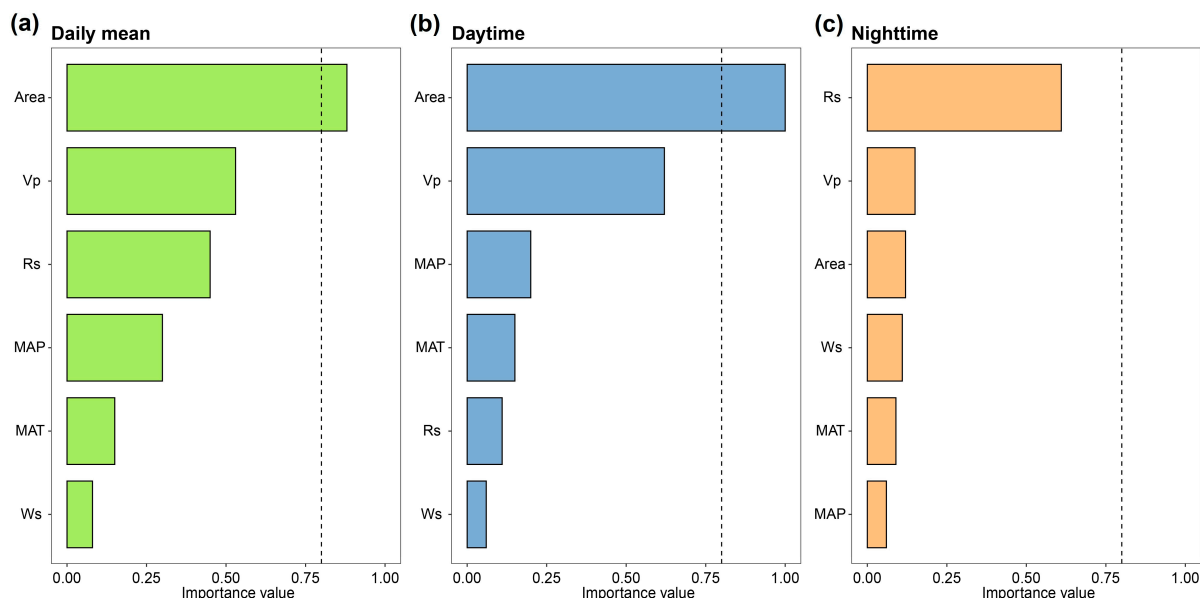


Figure 8. Importance of each predictor of the PV power plant effects, (a) daily mean, (b) daytime period, and (c) nighttime period. The importance value is based on the sum of Akaike weights derived from model selection using corrected Akaike’s information criteria. Cutoff is set at 0.8 (dash line) to differentiate between essential and nonessential predictors.

4. Discussion

4.1. PV Power Plant Effects on LST Vary between Day and Night

We found significant daytime cooling but nighttime warming effects of PV power plants in the Gobi Desert of China. However, because the daytime cooling surpasses the

nighttime warming, there was an overall cooling effect of PV power plants on the daily mean LST. The daytime cooling aligns with previous findings from Dunhuang [11], but the nighttime warming effect contradicts the result of Zhang and Xu [39] from various ecosystems. A possible reason for this discrepancy could be that our study took place in a certain ecosystem type, i.e., Gobi.

We attribute the daytime cooling effect of PV plants to the changes in albedo, shading, and the conversion of solar energy by PV panels [3,12,52]. Indeed, satellite-derived LST data are sensitive to the albedo [39]. Furthermore, our result showing a positive correlation between plant area and the daytime cooling effect (Figure 7b) is likely because larger areas have more shading and energy conversion.

On the other hand, the nighttime warming effect cannot be directly explained by albedo or energy conversion because there is no sunlight and PV generation at night. We posit that the warming results from shading by PV panels, which impedes nighttime cooling and induces warming. PV panels provide insulation and reduce radiation fluxes [52,53], hindering cooling. The existence of PV panels also reduces the wind speeds [30], which also limits cooling. Furthermore, the positive correlation between the nighttime PV plant effect and area but negative correlation with wind speed that we observed (Figure 7c) also indicates that the nighttime warming effect is associated with a reduction in heat dissipation. Finally, our observed positive correlation between annual precipitation and the warming effect (Figure 7c) may be because increased soil moisture under the panels [54], along with the higher heat capacity of water relative to the soil and gravel substrate in Gobi, reduces temperature within the PV plants.

4.2. PV Power Plant Effects on LSTs Vary between Seasons

We identified substantial seasonal variation in the effects of PV power plants on LST. Specifically, daytime cooling was most pronounced in spring and autumn, while nighttime warming was highest in spring. These results align with previous research [9,52] and are most likely due to changes in the climate across seasons. The efficiency of PV panels depends on ambient temperature [55]; it is necessary to consider the combination of temperature and light in different seasons. Despite higher radiation in the summer, milder spring and autumn temperatures improve PV efficiency, enhancing cooling. Likewise, higher humidity in the summer increases the environmental heat capacity, limiting nighttime warming compared to the spring, when it is drier. Considering the cumulative LST throughout the daytime and nighttime, we propose that constructing larger PV power plants in the wetter Gobi Desert will yield a more substantial LST cooling effect. Finally, in winter, larger solar angles lead to more panel shading, increasing cooling [52]. Colder temperatures during the winter also restrict nighttime warming.

4.3. Implications for the Management of PV Systems in Gobi Desert

As PV power plants continue to be deployed in the Gobi Desert, significant alterations in local microclimates are likely, with subsequent impacts on adjacent ecosystems [29,56]. Our results indicate that PV power plants reduce the local LST. Given the positive relationship between LST and evapotranspiration [57], the decrease in LST may lead to a reduction in evapotranspiration and, consequently, increases in soil humidity in the plant. At the same time, the decrease in surface soil carbon stock with warming [58] may be mitigated by the cooling effect of PV power plants in the Gobi Desert.

The combination of daytime cooling and nighttime warming from Gobi PV power plants might enhance vegetation growth. Temperature [59] and water availability [60] play crucial roles in plant growth in arid regions, where elevated daytime temperatures can trigger heat stress, hindering root growth and plant regeneration [61,62]. As a result, the moderation of LST of Gobi PV power plants can at least partially mitigate the extreme soil conditions (hot in the daytime, cold at night). This can increase water and nutrient content and utilization [63] and foster vegetation growth. However, cooling during the growing season (spring and summer) would also affect the phenology of vegetation [64].

Ultimately, a comprehensive understanding of the impacts of Gobi PV power plants on LST can provide valuable insights for informed decision-making regarding power plant siting, scale, design, and land management. Our study suggests that the cooling effects of PV power plants are scale-dependent, with larger installations causing more cooling. This is particularly important in the Gobi Deserts, where large-scale PV power plants are common. The effect on LST can be adjusted through design considerations. Adjustments in the dimensions, arrangement, elevation, orientation, and incline are all likely to amplify or diminish the PV plant effects on LST.

4.4. Uncertainties of Impact Analysis of PV on LST in Our Study

Our study makes two key contributions. First, by examining the 16 largest Gobi Desert PV plants in China, we advance understanding of extensive PV plant impacts on LST. Second, our expanded geographic scope across the Chinese Gobi Desert and our use of temporally matching conditions three years before and after installation and across day and night, where each PV plant has more than 1600 MOD/MYD daytime and nighttime data (Table S4), provides greater generality. In addition, the view zenith angle (VZA) could result in some uncertainties to MODIS LST data [65]. However, since our study mainly examines LST changes before and after PV plant construction and between internal and external areas, VZA-induced errors in these conditions will be resolved by comparing before and after construction and internal and external areas (Figure S4).

Nonetheless, our study has clear limitations. MODIS data do encompass inherent noise [66,67] and offer discrete point data at specific temporal intervals. In addition, there is inherent uncertainty in pinpointing and identifying PV power plant locations. Considering the swift expansion of PV power plants worldwide, we advocate that future research should prioritize the investigation of the environmental ramifications of these facilities across wider geographic extents and a diverse array of ecosystem types.

5. Conclusions

Utilizing satellite remote sensing data, we assessed alterations in the LST of the 16 largest PV power plants within China's Gobi Desert. Our findings reveal that the daily mean LST attributed to PV power plants manifests as an overall cooling effect, albeit with both diurnal and seasonal fluctuations. That is, there is a cooling effect during the daytime of -0.69 ± 0.10 °C and a warming effect during the nighttime of 0.22 ± 0.05 °C. The most pronounced cooling effect is during autumn, whereas the most substantial warming effect is during spring. Further analysis demonstrates that the cooling effect is predominantly associated with the area and water vapor pressure. Our methodology can be extended to examine the environmental repercussions of PV power plants across geographical regions, encompass diverse ecosystem types, and employ a broader spectrum of indicators. Such expansion will enrich our comprehension of the environmental effects arising from the construction of PV power plants, offering valuable insights for fostering sustainable development and strategic planning in the realm of clean energy.

Supplementary Materials: The following supporting information can be downloaded at: <https://www.mdpi.com/article/10.3390/rs16101711/s1>, Figure S1: The utilization of LST data from the largest and smallest plants in terms of area; Figure S2: Effects of photovoltaic power plant on land surface temperature in Dunhuang power plant; Figure S3: Effects of the Dunhuang PV power plant on land surface temperature; Figure S4: Elimination of view zenith angle error; Table S1: Detailed information of photovoltaic power plants in the Gobi Desert of China; Table S2: Potential impact factors and their resources of each photovoltaic power plant; Table S3: The *p*-value of model averaging after model selection in each period; Table S4: The data quantity of each PV plant.

Author Contributions: Conceptualization, X.W. (Xinxin Wang) and J.W.; methodology, X.W. (Xubang Wang), X.L. and X.W. (Xinxin Wang); writing—original draft preparation, X.W. (Xubang Wang) and X.W. (Xinxin Wang); writing—review and editing, X.W. (Xubang Wang), X.W. (Xinxin Wang), Q.Z., Y.Z., X.L., J.L., S.C. and J.W. All authors have read and agreed to the published version of the manuscript.

Funding: This work was supported by the Talent Scientific Fund of Lanzhou University, the Gansu Provincial Key Program of Science Fund (22JR5RA396) and Fundamental Research Funds for the Central Universities (lzujbky-2021-sp51).

Data Availability Statement: The raw data supporting the conclusions of this article will be made available by the authors on request.

Acknowledgments: The authors express their heartfelt gratitude to the editors and reviewers for their diligent efforts in facilitating the publication of this paper.

Conflicts of Interest: The authors declare no conflicts of interest.

References

- Intergovernmental Panel on Climate Change (IPCC). *Ar6 Synthesis Report: Climate Change 2023*; IPCC: Geneva, Switzerland, 2023.
- Tawalbeh, M.; Al-Othman, A.; Kafiah, F.; Abdelsalam, E.; Almomani, F.; Alkasrawi, M. Environmental Impacts of Solar Photovoltaic Systems: A Critical Review of Recent Progress and Future Outlook. *Sci. Total. Environ.* **2020**, *759*, 143528. [[CrossRef](#)]
- Hu, A.; Levis, S.; Meehl, G.A.; Han, W.; Washington, W.M.; Oleson, K.W.; van Ruijven, B.J.; He, M.; Strand, W.G. Impact of Solar Panels on Global Climate. *Nat. Clim. Chang.* **2015**, *6*, 290–294. [[CrossRef](#)]
- Li, Z. Prospects of Photovoltaic Technology. *Engineering* **2023**, *21*, 28–31. [[CrossRef](#)]
- Kruitwagen, L.; Story, K.T.; Friedrich, J.; Byers, L.; Skillman, S.; Hepburn, C. A Global Inventory of Photovoltaic Solar Energy Generating Units. *Nature* **2021**, *598*, 604–610. [[CrossRef](#)]
- Dong, H.; Zeng, B.; Wang, Y.; Liu, Y.; Zeng, M. China's Solar Subsidy Policy: Government Funding Yields to Open Markets. *IEEE Power Energy Mag.* **2020**, *18*, 49–60. [[CrossRef](#)]
- Zhang, N.; Duan, H.; Shan, Y.; Miller, T.R.; Yang, J.; Bai, X. Booming Solar Energy is Encroaching on Cropland. *Nat. Geosci.* **2023**, *16*, 932–934. [[CrossRef](#)]
- Hernandez, R.R.; Armstrong, A.; Burney, J.; Ryan, G.; Moore-O'leary, K.; Diédhiou, I.; Grodsky, S.M.; Saul-Gershenz, L.; Davis, R.; Macknick, J.; et al. Techno-Ecological Synergies of Solar Energy for Global Sustainability. *Nat. Sustain.* **2019**, *2*, 560–568. [[CrossRef](#)]
- Chang, R.; Luo, Y.; Zhu, R. Simulated Local Climatic Impacts of Large-Scale Photovoltaics over the Barren Area of Qinghai, China. *Renew. Energy* **2020**, *145*, 478–489. [[CrossRef](#)]
- Li, Y.; Kalnay, E.; Motescharrei, S.; Rivas, J.; Kucharski, F.; Kirk-Davidoff, D.; Bach, E.; Zeng, N. Climate Model Shows Large-Scale Wind and Solar Farms in the Sahara Increase Rain and Vegetation. *Science* **2018**, *361*, 1019–1022. [[CrossRef](#)]
- Hua, Y.; Chai, J.; Chen, L.; Liu, P. The Influences of the Desert Photovoltaic Power Station on Local Climate and Environment: A Case Study in Dunhuang Photovoltaic Industrial Park, Dunhuang City, China in 2019. *Atmosphere* **2022**, *13*, 1235. [[CrossRef](#)]
- Armstrong, A.; Waldron, S.; Whitaker, J.; Ostle, N.J. Wind Farm and Solar Park Effects on Plant-Soil Carbon Cycling: Uncertain Impacts of Changes in Ground-Level Microclimate. *Glob. Chang. Biol.* **2014**, *20*, 1699–1706. [[CrossRef](#)]
- Hastik, R.; Basso, S.; Geitner, C.; Haida, C.; Poljanec, A.; Portaccio, A.; Vrščaj, B.; Walzer, C. Renewable Energies and Ecosystem Service Impacts. *Renew. Sustain. Energy Rev.* **2015**, *48*, 608–623. [[CrossRef](#)]
- Holland, R.A.; Scott, K.; Agnolucci, P.; Rapti, C.; Eigenbrod, F.; Taylor, G. The Influence of the Global Electric Power System on Terrestrial Biodiversity. *Proc. Natl. Acad. Sci. USA* **2019**, *116*, 26078–26084. [[CrossRef](#)]
- Zhang, H.; Wang, E.; Zhou, D.; Luo, Z.; Zhang, Z. Rising Soil Temperature in China and Its Potential Ecological Impact. *Sci. Rep.* **2016**, *6*, 35530. [[CrossRef](#)] [[PubMed](#)]
- Guoqing, L.; Hernandez, R.R.; Blackburn, G.A.; Davies, G.; Hunt, M.; Whyatt, J.D.; Armstrong, A. Ground-Mounted Photovoltaic Solar Parks Promote Land Surface Cool Islands in Arid Ecosystems. *Renew. Sustain. Energy Transit.* **2021**, *1*, 100008. [[CrossRef](#)]
- García-García, A.; Cuesta-Valero, F.J.; Miralles, D.G.; Mahecha, M.D.; Quaas, J.; Reichstein, M.; Zscheischler, J.; Peng, J. Soil Heat Extremes Can Outpace Air Temperature Extremes. *Nat. Clim. Chang.* **2023**, *13*, 1237–1241. [[CrossRef](#)]
- Li, Z.-L.; Tang, B.-H.; Wu, H.; Ren, H.; Yan, G.; Wan, Z.; Trigo, I.F.; Sobrino, J.A. Satellite-Derived Land Surface Temperature: Current Status and Perspectives. *Remote Sens. Environ.* **2013**, *131*, 14–37. [[CrossRef](#)]
- Lu, L.; Zhang, T.; Wang, T.; Zhou, X. Evaluation of Collection-6 MODIS Land Surface Temperature Product Using Multi-Year Ground Measurements in an Arid Area of Northwest China. *Remote Sens.* **2018**, *10*, 1852. [[CrossRef](#)]
- Armstrong, A.; Ostle, N.J.; Whitaker, J. Solar Park Microclimate and Vegetation Management Effects on grassland Carbon Cycling. *Environ. Res. Lett.* **2016**, *11*, 074016. [[CrossRef](#)]
- Chang, R.; Shen, Y.; Luo, Y.; Wang, B.; Yang, Z.; Guo, P. Observed Surface Radiation and Temperature Impacts from the Large-scale Deployment of Photovoltaics in the Barren Area of Gonghe, China. *Renew. Energy* **2018**, *118*, 131–137. [[CrossRef](#)]
- Vervloesem, J.; Marcheggiani, E.; Choudhury, A.M.; Muys, B. Effects of Photovoltaic Solar Farms on Microclimate and Vegetation Diversity. *Sustainability* **2022**, *14*, 7493. [[CrossRef](#)]
- Luo, L.; Zhuang, Y.; Liu, H.; Zhao, W.; Chen, J.; Du, W.; Gao, X. Environmental Impacts of Photovoltaic Power Plants in Northwest China. *Sustain. Energy Technol. Assess.* **2023**, *56*, 103120. [[CrossRef](#)]
- Wu, Z.; Hou, A.; Chang, C.; Huang, X.; Shi, D.; Wang, Z. Environmental Impacts of Large-Scale CSP Plants in Northwestern China. *Environ. Sci. Process. Impacts* **2014**, *16*, 2432–2441. [[CrossRef](#)]

25. Broadbent, A.M.; Krayenhoff, E.S.; Georgescu, M.; Sailor, D.J. The Observed Effects of Utility-Scale Photovoltaics on Near-Surface Air Temperature and Energy Balance. *J. Appl. Meteorol. Clim.* **2019**, *58*, 989–1006. [[CrossRef](#)]
26. Jin, Y.; Hu, S.; Ziegler, A.D.; Gibson, L.; Campbell, J.E.; Xu, R.; Chen, D.; Zhu, K.; Zheng, Y.; Ye, B.; et al. Energy Production and Water Savings from Floating Solar Photovoltaics on Global Reservoirs. *Nat. Sustain.* **2023**, *6*, 865–874. [[CrossRef](#)]
27. Zhang, Y.; Tian, Z.; Liu, B.; Chen, S.; Wu, J. Effects of Photovoltaic Power Station Construction on Terrestrial Ecosystems: A Meta-Analysis. *Front. Ecol. Evol.* **2023**, *11*, 1151182. [[CrossRef](#)]
28. Choi, C.S.; Macknick, J.; Li, Y.; Bloom, D.; McCall, J.; Ravi, S. Environmental Co-Benefits of Maintaining Native Vegetation with Solar Photovoltaic Infrastructure. *Earth's Futur.* **2023**, *11*, e2023EF003542. [[CrossRef](#)]
29. Wu, C.; Liu, H.; Yu, Y.; Zhao, W.; Liu, J.; Yu, H.; Yetemen, O. Ecohydrological Effects of Photovoltaic Solar Farms on Soil Microclimates and Moisture Regimes in Arid Northwest China: A Modeling Study. *Sci. Total. Environ.* **2021**, *802*, 149946. [[CrossRef](#)]
30. Chang, R.; Yan, Y.; Wu, J.; Wang, Y.; Gao, X. Projected PV Plants in China's Gobi Deserts Would Result in Lower Evaporation and Wind. *Sol. Energy* **2023**, *256*, 140–150. [[CrossRef](#)]
31. Li, Z.; Zhao, Y.; Luo, Y.; Yang, L.; Li, P.; Jin, X.; Jiang, J.; Liu, R.; Gao, X. A Comparative Study on the Surface Radiation Characteristics of Photovoltaic Power Plant in the Gobi desert. *Renew. Energy* **2021**, *182*, 764–771. [[CrossRef](#)]
32. Xia, Z.; Li, Y.; Chen, R.; Sengupta, D.; Guo, X.; Xiong, B.; Niu, Y. Mapping the Rapid Development of Photovoltaic Power Stations in Northwestern China Using Remote Sensing. *Energy Rep.* **2022**, *8*, 4117–4127. [[CrossRef](#)]
33. Wang, J.; Chen, L.; Tan, Z.; Du, E.; Liu, N.; Ma, J.; Sun, M.; Li, C.; Song, J.; Lu, X.; et al. Inherent Spatiotemporal Uncertainty of Renewable Power in China. *Nat. Commun.* **2023**, *14*, 5379. [[CrossRef](#)] [[PubMed](#)]
34. Lu, H.; Wang, X.; Wang, X.; Chang, X.; Zhang, H.; Xu, Z.; Zhang, W.; Wei, H.; Zhang, X.; Yi, S.; et al. Formation and Evolution of Gobi Desert in Central and Eastern Asia. *Earth-Sci. Rev.* **2019**, *194*, 251–263. [[CrossRef](#)]
35. Yao, Z.; Xiao, J.; Ma, X. The Impact of Large-Scale Afforestation on Ecological Environment in the Gobi Region. *Sci. Rep.* **2021**, *11*, 14383. [[CrossRef](#)] [[PubMed](#)]
36. Chang, R.; Yan, Y.; Luo, Y.; Xiao, C.; Wu, C.; Jiang, J.; Shi, W. A Coupled WRF-PV Mesoscale Model Simulating the Near-Surface Climate of Utility-Scale Photovoltaic Plants. *Sol. Energy* **2022**, *245*, 278–289. [[CrossRef](#)]
37. Qin, Y.; Li, Y.; Xu, R.; Hou, C.; Armstrong, A.; Bach, E.; Wang, Y.; Fu, B. Impacts of 319 Wind Farms on Surface Temperature and Vegetation in the United States. *Environ. Res. Lett.* **2022**, *17*, 024026. [[CrossRef](#)]
38. Wu, D.; Grodsky, S.M.; Xu, W.; Liu, N.; Almeida, R.M.; Zhou, L.; Miller, L.M.; Roy, S.B.; Xia, G.; Agrawal, A.A.; et al. Observed Impacts of Large Wind Farms on Grassland Carbon Cycling. *Sci. Bull.* **2023**, *68*, 2889–2892. [[CrossRef](#)]
39. Zhang, X.; Xu, M. Assessing the Effects of Photovoltaic Powerplants on Surface Temperature Using Remote Sensing Techniques. *Remote Sens.* **2020**, *12*, 1825. [[CrossRef](#)]
40. Justice, C.; Townshend, J.; Vermote, E.; Masuoka, E.; Wolfe, R.; Saleous, N.; Roy, D.; Morisette, J. An Overview of MODIS Land Data Processing and Product Status. *Remote Sens. Environ.* **2002**, *83*, 3–15. [[CrossRef](#)]
41. Phan, T.N.; Kappas, M. Application of MODIS Land Surface Temperature Data: A Systematic Literature Review and Analysis. *J. Appl. Remote Sens.* **2018**, *12*, 041501. [[CrossRef](#)]
42. Wang, K.; Wan, Z.; Wang, P.; Sparrow, M.; Liu, J.; Haginoya, S. Evaluation and Improvement of the MODIS Land Surface Temperature/Emissivity Products Using Ground-Based Measurements at a Semi-Desert Site on the Western Tibetan Plateau. *Int. J. Remote Sens.* **2007**, *28*, 2549–2565. [[CrossRef](#)]
43. Wan, Z.; Hook, S.; Hulley, G. *Modis/Terra Land Surface Temperature/Emissivity Daily L3 Global 1 km Sin Grid V061*; NASA EOSDIS Land Processes Distributed Active Archive Center: Sioux Falls, SD, USA, 2021.
44. Wan, Z.; Hook, S.; Hulley, G. *Modis/Aqua Land Surface Temperature/Emissivity Daily L3 Global 1 km Sin Grid V061*; NASA EOSDIS Land Processes Distributed Active Archive Center: Sioux Falls, SD, USA, 2021.
45. Fick, S.E.; Hijmans, R.J. WorldClim 2: New 1-km spatial Resolution Climate Surfaces for Global land Areas. *Int. J. Climatol.* **2017**, *37*, 4302–4315. [[CrossRef](#)]
46. Python Software Foundation. *Python Documentation, version 3.12.0*; Python Software Foundation: Wilmington, DE, USA, 2023.
47. Google Earth Pro, version 7. 3.6; Google LLC: Mountain View, CA, USA, 2022.
48. Zhou, L.; Tian, Y.; Roy, S.B.; Thorncroft, C.; Bosart, L.F.; Hu, Y. Impacts of Wind Farms on Land Surface Temperature. *Nat. Clim. Chang.* **2012**, *2*, 539–543. [[CrossRef](#)]
49. R: A Language and Environment for Statistical Computing. version 4.3.2; R Foundation for Statistical Computing: Vienna, Austria, 2013.
50. Gelman, A. Scaling Regression Inputs by Dividing by Two Standard Deviations. *Stat. Med.* **2007**, *27*, 2865–2873. [[CrossRef](#)]
51. Grueber, C.E.; Nakagawa, S.; Laws, R.J.; Jamieson, I.G. Multimodel Inference in Ecology and Evolution: Challenges and Solutions. *J. Evol. Biol.* **2011**, *24*, 699–711. [[CrossRef](#)]
52. Yang, L.; Gao, X.; Lv, F.; Hui, X.; Ma, L.; Hou, X. Study on the Local Climatic Effects of Large Photovoltaic Solar Farms in Desert Areas. *Sol. Energy* **2017**, *144*, 244–253. [[CrossRef](#)]
53. Barron-Gafford, G.A.; Pavao-Zuckerman, M.A.; Minor, R.L.; Sutter, L.F.; Barnett-Moreno, I.; Blackett, D.T.; Thompson, M.; Dimond, K.; Gerlak, A.K.; Nabhan, G.P.; et al. Agrivoltaics Provide Mutual Benefits across the Food–Energy–Water Nexus in Drylands. *Nat. Sustain.* **2019**, *2*, 9848–9855. [[CrossRef](#)]

54. Wu, W.; Yue, S.; Zhou, X.; Guo, M.; Wang, J.; Ren, L.; Yuan, B. Observational Study on the Impact of Large-Scale Photovoltaic Development in Deserts on Local Air Temperature and Humidity. *Sustainability* **2020**, *12*, 3403. [[CrossRef](#)]
55. Rahman, M.; Hasanuzzaman, M.; Rahim, N. Effects of Various Parameters on PV-Module Power and Efficiency. *Energy Convers. Manag.* **2015**, *103*, 348–358. [[CrossRef](#)]
56. Liu, Y.; Zhang, R.; Huang, Z.; Cheng, Z.; López-Vicente, M.; Ma, X.; Wu, G. Solar Photovoltaic Panels Significantly Promote Vegetation Recovery by Modifying the Soil Surface Microhabitats in an Arid Sandy Ecosystem. *Land Degrad. Dev.* **2019**, *30*, 2177–2186. [[CrossRef](#)]
57. Sun, Z.; Wang, Q.; Batkhisig, O.; Ouyang, Z. Relationship between Evapotranspiration and Land Surface Temperature under Energy- and Water-Limited Conditions in Dry and Cold Climates. *Adv. Meteorol.* **2015**, *2016*, 1835487. [[CrossRef](#)]
58. Wang, M.; Guo, X.; Zhang, S.; Xiao, L.; Mishra, U.; Yang, Y.; Zhu, B.; Wang, G.; Mao, X.; Qian, T.; et al. Global Soil Profiles Indicate Depth-Dependent Soil Carbon Losses under a Warmer Climate. *Nat. Commun.* **2022**, *13*, 5514. [[CrossRef](#)] [[PubMed](#)]
59. Beedlow, P.A.; Lee, E.H.; Tingey, D.T.; Waschmann, R.S.; Burdick, C.A. The Importance of Seasonal Temperature and Moisture Patterns on Growth of Douglas-Fir in Western Oregon, USA. *Agric. For. Meteorol.* **2013**, *169*, 174–185. [[CrossRef](#)]
60. Zhou, X.; Zhang, Y.; Ji, X.; Downing, A.; Serpe, M. Combined Effects of Nitrogen Deposition and Water Stress on Growth and Physiological Responses of Two Annual Desert Plants in Northwestern China. *Environ. Exp. Bot.* **2011**, *74*, 1–8. [[CrossRef](#)]
61. Walck, J.L.; Hidayati, S.N.; Dixon, K.W.; Thompson, K.; Poschlod, P. Climate Change and Plant Regeneration from Seed. *Glob. Chang. Biol.* **2010**, *17*, 2145–2161. [[CrossRef](#)]
62. Nishar, A.; Bader, M.K.-F.; O’gorman, E.J.; Deng, J.; Breen, B.; Leuzinger, S. Temperature Effects on Biomass and Regeneration of Vegetation in a Geothermal Area. *Front. Plant Sci.* **2017**, *8*, 249. [[CrossRef](#)] [[PubMed](#)]
63. Belnap, J. Surface Disturbances: Their Role in Accelerating Desertification. *Environ. Monit. Assess.* **1995**, *37*, 39–57. [[CrossRef](#)] [[PubMed](#)]
64. Marrou, H.; Guilioni, L.; Dufour, L.; Dupraz, C.; Wery, J. Microclimate under Agrivoltaic Systems: Is Crop Growth Rate Affected in the Partial Shade of Solar Panels? *Agric. For. Meteorol.* **2013**, *177*, 117–132. [[CrossRef](#)]
65. Bao, Y.; Chen, S.; Liu, Q.; Xiao, Q.; Cao, C. Land Surface Temperature and Emissivity Retrieval by Integrating MODIS Data Onboard Terra and Aqua Satellites. *Int. J. Remote Sens.* **2011**, *32*, 1449–1469. [[CrossRef](#)]
66. Wan, Z. New Refinements and Validation of the MODIS Land-Surface Temperature/Emissivity Products. *Remote Sens. Environ.* **2008**, *112*, 59–74. [[CrossRef](#)]
67. Wan, Z.; Zhang, Y.; Zhang, Q.; Li, Z.L. Quality Assessment and Validation of the MODIS Global land Surface Temperature. *Int. J. Remote Sens.* **2004**, *25*, 261–274. [[CrossRef](#)]

Disclaimer/Publisher’s Note: The statements, opinions and data contained in all publications are solely those of the individual author(s) and contributor(s) and not of MDPI and/or the editor(s). MDPI and/or the editor(s) disclaim responsibility for any injury to people or property resulting from any ideas, methods, instructions or products referred to in the content.